Synergy of Pickering Emulsion and Sol-Gel Process for the Construction of an Efficient, Recyclable Enzyme Cascade System

Jiafu Shi, Xiaoli Wang, Wenyan Zhang, Zhongyi Jiang, Yanpeng Liang, Yuanyuan Zhu, and Chunhong Zhang*

An efficient, easily recyclable enzyme cascade system based on nanoparticle-stabilized capsules (NPSCs) is constructed through a synergy of a Pickering emulsion and sol-gel process. Specifically, oligodopa-coated titania nanoparticles (biomimetic titania) containing the first enzyme (FateDH) are synthesized through a bioadhesion-assisted biomimetic mineralization approach. The biomimetic titania is then spontaneously assembled at the interface between the oil phase (hexadecane/butyl titanate (BuTi) mixture) and water phase during the formation of Pickering emulsions. The sol-gel process of BuTi can produce not only butanol for assisting the formation of Pickering emulsions but also titania gel particles (sol-gel titania) for cross-linking the biomimetic titania through catechol-titanium chelating. The NPSCs obtained, which contain the first enzyme, conjugate the second enzyme (FaldDH) onto the surface for constructing the enzyme cascade system. The system exhibits high activity and stability, particularly, superior recyclability for conversion of CO_2 into formaldehyde. In detail, the system shows a formaldehyde yield of 50.0%, and can quickly float onto the air/water interface soon after stopping the agitation of reaction mixtures, which ensures that the formaldehyde yield keeps almost unaltered after 10 times recycling. This study will be useful for facile construction of a wealth of catalytic systems with efficient, recyclable attributes.

1. Introduction

Enzymes can catalyze a broad range of reactions with exquisite stereo-specificity, regio- and chemo-selectivity,[1–4] and have been working as a powerful tool for chemical synthesis,[5,6] biosensors,[7,8] biofuel cells,[9] and so on. However, the application of free enzymes in industry is often hampered by their low operational stability and poor recyclability.[10,11] Fortunately, the enzyme immobilization technique has shown great promise to solve these problems.

Dr. J. F. Shi, Dr. X. L. Wang, W. Y. Zhang,
Prof. Z. Y. Jiang, Y. P. Liang, Y. Y. Zhu, C. H. Zhang
Key Laboratory for Green Chemical Technology
of Ministry of Education
School of Chemical Engineering and Technology
Tianjin University
Tianjin 300072, China
E-mail: zhyjiang@tju.edu.cn

DOI: 10.1002/adfm.201202068

Among the existing enzyme immobilization approaches,[1,12] sol-gel encapsulation has become increasingly popular owing to its facile and controllable process, low operation temperature, low cost and easy attainability of raw materials, etc.[13,14] In addition, the resultant inorganic gels often exhibit high enzyme loading capacity, excellent pH stability and thermal stability.[12,13,15] Until now, the sol-gel scaffolds primarily used for enzyme encapsulation include glass monoliths and nanoparticles (NPs). In recent years, numerous efforts have focused on preparing sol-gel NPs for enzyme encapsulation. This is mainly because the large specific surface area and small size of the NPs can increase enzyme loading capacity and particle mobility, reduce diffusion resistance and thus retain the inherent enzyme catalytic activity.[16–19] One of the first investigations about sol-gel encapsulation of enzymes within NPs was reported by Jain et al.[16] To obtain the sol-gel NPs, they have incorporated a water-in-oil microemulsion process into the traditional sol-gel process, which was conducted via the acid catalyzed hydrolysis and polycondensation of silicon alkoxides. To avoid enzyme denaturation by the harsh conditions and released alcohol, Cellesi et al.[20] have modified the sol-gel encapsulation approach by adding the buffer solution and evaporating the hydrolyzed tetraethyl orthosilicate. As far as we know, in the ocean, diatom utilizes protein scaffolds to catalyze silicate to form silica NPs under ambient conditions. Inspired by this, biomimetic mineralization processes have emerged as a versatile tool for generating excellent supports for enzyme immobilization. The mild and controllable reaction condition associated with biomineral NP formation is extremely favorable for enzyme encapsulation and enzyme activity retention.[17] In 2004, Luckarift et al.[14] first exploited a biomimetic approach to encapsulate butyrylcholinesterase through R5 peptide induced silicification. The biosilica support acquired a high enzyme encapsulation efficiency (>90%) and zero enzyme leaching. Moreover, the immobilized enzyme was much more stable than the free enzyme. Since then, a broad number of enzymes, including catalase,[21] β-galactosidase,[22]

alcohol dehydrogenase,[23] etc. have been successfully entrapped into the biomineral NPs especially silica or titania. Since NPs have a small size (≈25–500 nm) and a similar density to water, the recovery of NPs after the reaction becomes a difficult task. To the best of our knowledge, the commonly used strategy for recovering NPs is centrifugation, sometimes combined with filtration. However, the recovery efficiency is often very low unless the centrifugation speed reaches an extremely high value (>10 000 rpm).[14,22] As an energy-efficient process, magnetic separation has been recently developed, where NPs can be reused without significant loss of activity for a number of cycles.[24] Nevertheless, this approach is severely limited by the available magnetic materials, and is not applicable to the biomineral NPs such as silica or titania.

In general, when designing a "robust" immobilization approach, noncatalytic needs (separation, reuse, downstream processing, etc.) as well as catalytic needs (productivity, space-time yield, stability and selectivity, etc.) should be considered simultaneously.[1,25] Therefore, developing an efficient and recyclable enzyme support is highly desired for many biocatalytic processes.

In recent years, Pickering emulsions, a kind of oil/water or water/oil emulsions stabilized by NPs,[26,27] have attracted a surge of interest.[28–33] Until now, many kinds of NP stabilizers including silica, titania, clay and organic materials have been reported.[33–37] Theoretically, the placement of NPs at the oil/water or water/oil interface could lead to a decrease of energy of the system. The decrease of total free energy is much larger than that of thermal energy (k_B), which leads to a nearly permanent confinement of NPs to the interface.[38] To acquire stable Pickering emulsions, the wettability of NPs is crucial; this determines whether the emulsion is a water-in-oil or oil-in-water type. Quite often, relatively hydrophilic particles tend to stabilize oil-in-water emulsions. Locking NPs adsorbed on oil-in-water emulsion droplets can generate micrometer-sized, robust capsules enclosed by a thin nanoparticle layer,[39–42] which may offer a novel and generic approach to recover the NPs without dramatically changing their unique property.

In the present study, a facile approach, which uses a synergy between Pickering emulsion and sol-gel process, is developed to prepare nanoparticle-stabilized capsules (NPSCs) for constructing an efficient and recyclable enzyme cascade system. Specifically, the oligodopa-coated titania NPs (biomimetic titania) are synthesized through a bioadhesion-assisted biomimetic mineralization approach. A Pickering emulsion is formed by mixing the biomimetic titania with an oil (hexadecane/butyl titanate (BuTi) mixture)-water mixture through vigorous shaking. BuTi, as the inorganic precursor, produces butanol and titania gel particles (sol-gel titania) through the sol-gel process. Butanol can assist the formation of Pickering emulsions, while the sol-gel titania can cross-link the biomimetic titania through catechol-titanium chelation. The morphologies of the NPSCs can be tailored by varying the concentration of BuTi. To construct the enzyme cascade system, two enzymes are respectively immobilized through physical entrapment in the capsule wall and chemical conjugation on the capsule surface. The advantages of this approach may be realized in the following aspects: 1) the biomimetic titania NPs could spread on the surface of the oil droplets nearly in the form of a monolayer, which preserves their structure well; 2) the density difference between oil-containing capsules and water makes the NPSCs quickly float onto the air/water interface soon after stirring or shaking ceases, which makes recycling easier. Therefore, this system displays high catalytic activity and stability, as well as superior recyclability. As an example, an enzyme cascade system containing formate dehydrogenase (FateDH, the first enzyme) and formaldehyde dehydrogenase (FaldDH, the second enzyme) is explored for converting CO_2 to formaldehyde.

2. Results and Discussion

2.1. Synthesis and Morphology Control of the Nanoparticle-Stabilized Capsules (NPSCs)

The NPSCs were fabricated through the synergy between Pickering emulsion and sol-gel process as illustrated in **Scheme 1**. The whole process can be divided into two steps: 1) emulsification of the oil-water mixture to form oil-in-water emulsions; 2) sol-gel process of butyl titanate (BuTi) to produce a thin layer of titania gel particles (sol-gel titania) and butanol at the oil/water interface. Adsorption of butanol on the oligodopa-coated titania nanoparticles (biomimetic titania) induced the self-assembly of the biomimetic titania at the oil/water interface (formation of Pickering emulsions). Meanwhile, the sol-gel titania was the indispensable constituent in the formation of an intact and robust capsule wall (formation of the NPSCs). Interestingly, in the second step, it was found that the biomimetic titania was not able to self-assemble at the hexadecane/water interface (Figure S1a and S1b, Supporting Information). Therefore, it can be deduced that BuTi played a critical role in the formation of a stable Pickering emulsion. It is known that, once in contact with water, BuTi can be hydrolyzed into titanate and butanol within minutes. It could be hypothesized that butanol can alter the surface wettability of the biomimetic titania and enhance their stability at the oil/water interface. To test this hypothesis, the wettability of the biomimetic titania/water/oil three-phase system with and without butanol in the oil phase (**Figure 1**a) was studied. For oil without butanol (Figure 1c), the

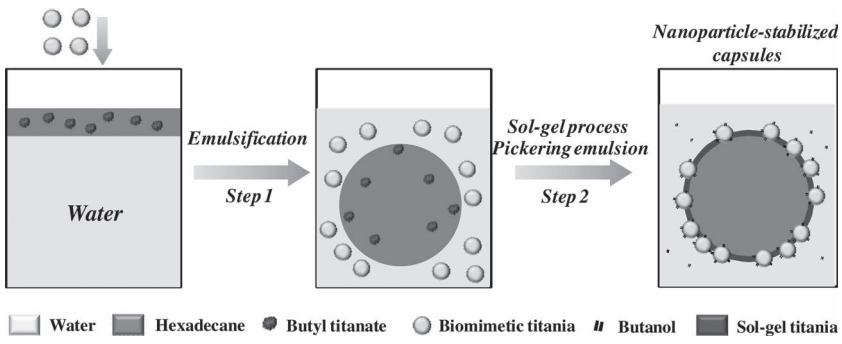

Scheme 1. Schematic preparation procedure of nanoparticle-stabilized capsules (NPSCs).

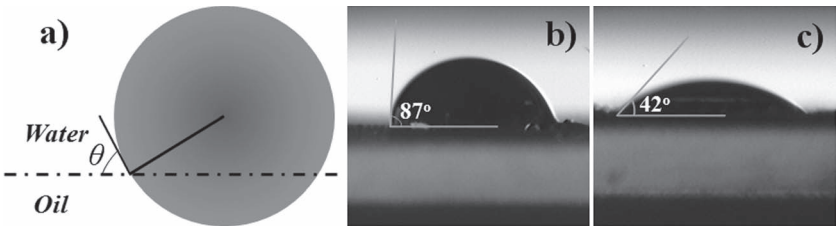

Figure 1. a) Scheme of an isotropic particle at the oil/water interface. b,c) Photographs of a 5 μL water droplet, resting on the surface of a thin film of the biomimetic titania, which was transferred from b) the hexadecane/air interface on a glass slide and c) the oil (hexadecane/butanol mixture)/air interface on a glass slide.[29,43] Note that the contact angles in Figure 1b,c reflect the contact angles (θ) of the biomimetic titania at the hexadecane/water interface and the oil/water interface, respectively.[29,43]

contact angle was ca. 42°, demonstrating that oil had a much weaker affinity toward the biomimetic titania than water. This situation was changed significantly in the presence of butanol. It was found that the contact angle between the oil film at the biomimetic titania and a drop of water was ca. 87° (Figure 1b). Normally, the physically aggregated biomimetic titania would detach from the oil/water interface if the shear stress was high enough. In our study, the tight connections among the biomimetic titania and thus the robust, intact capsule wall should be ascribed to the cross-linking of sol-gel titania via the polycondensation of titanate. Specifically, as shown in Figure S2a (Supporting Information), the surface of the biomimetic titania was covered with oligodopa, which is rich in free catechol groups.[44] The titanium atom in sol-gel titania could be chelated by catechol groups to form metal-organic coordination bonds.

To elucidate the morphological influence of BuTi in this process, the NPSCs were prepared from different BuTi/oil ratios and characterized by an optical camera, scanning electron microscope (SEM) and energy dispersive spectroscope (EDS). It is noteworthy to mention that the NPSCs synthesized with 1.25, 3.75, 6.25, and 12.5 μL of BuTi were denoted as NPSCs-1, NPSCs-2, NPSCs-3, and NPSCs-4, respectively. After dropping 20 μL of the solution containing NPSCs-1, NPSCs-2, NPSCs-3 or NPSCs-4 onto a glass slide, spherical capsules could be observed, indicating successful preparation of the NPSCs. With an increase in the BuTi amount, the diameters of the NPSCs decreased slightly as shown in **Figure 2**a–c. Moreover, the morphologies of the lyophilized NPSCs were also observed by SEM. NPSCs-1 with broken structures were obtained as shown in Figure 2d, while NPSCs-2 and NPSCs-3 displayed typical capsular morphology (Figure 2e,f). Furthermore, distinct differences also existed between NPSCs-2 and NPSCs-3. NPSCs-2 were tiled on the glass slide, while NPSCs-3 exhibited a spherical hollow structure without collapse. Such results could be interpreted in the following manner: more BuTi would produce a larger amount of sol-gel titania so as to form a more robust capsule wall, which was confirmed by the EDS results in **Figure 3**a–c. Additionally, as illustrated in Figure 3d, once the amount of BuTi increased to 12.5 μL, NPSCs-4 would be formed accompanied by plenty of sol-gel titania in the free form.

In order to explore the nanostructure of the NPSCs, HR-SEM images of NPSCs-2 and NPSCs-3 were acquired. For NPSCs-2, it could be observed that the NPs were uniformly distributed on the capsule wall (**Figure 4**a). These NPs should originate from the added biomimetic titania, since the NPSCs could not be formed in the absence of the biomimetic titania. As compared to NPSCs-2, NPSCs-3 possessed a continuous capsule wall, where NPs could not be distinguished clearly and may be fully entrapped in the capsule wall (Figure 4b). NPSCs-2 with intact capsular morphology and a high exposure of the biomimetic titania were then selected for the subsequent construction of the enzyme cascade system.

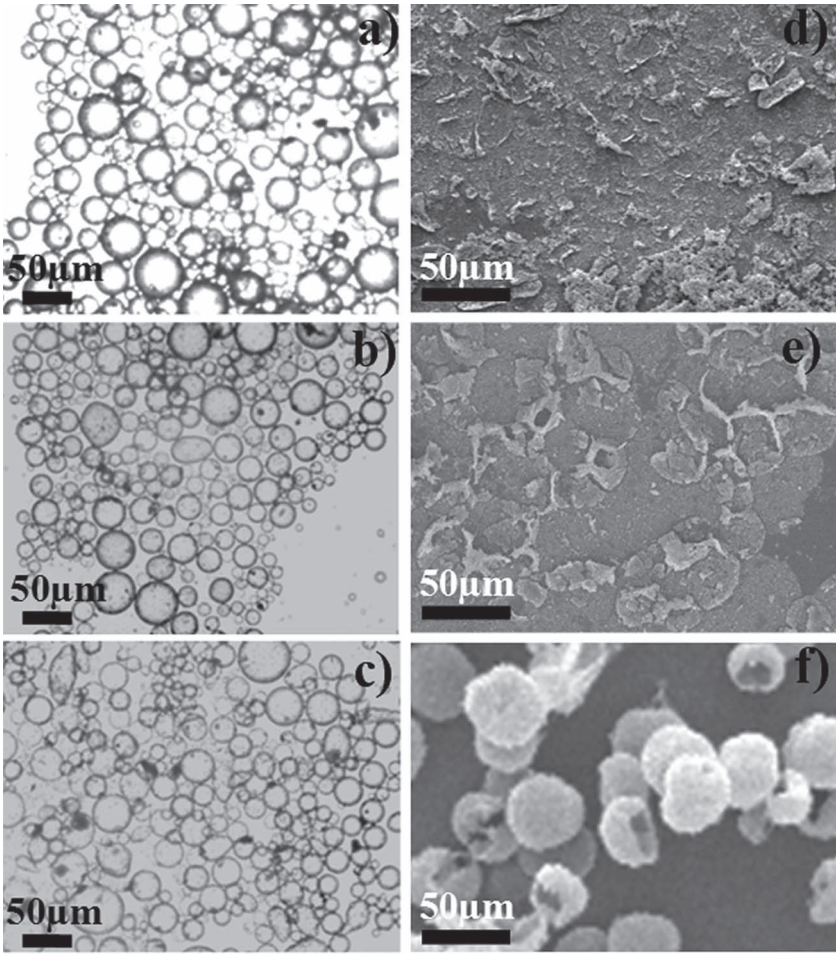

Figure 2. a–c) Optical micrographs and d–f) SEM images of the NPSCs: a,d) NPSCs-1, b,e) NPSCs-2, c,f) NPSCs-3 (scale bar: 50 μm).

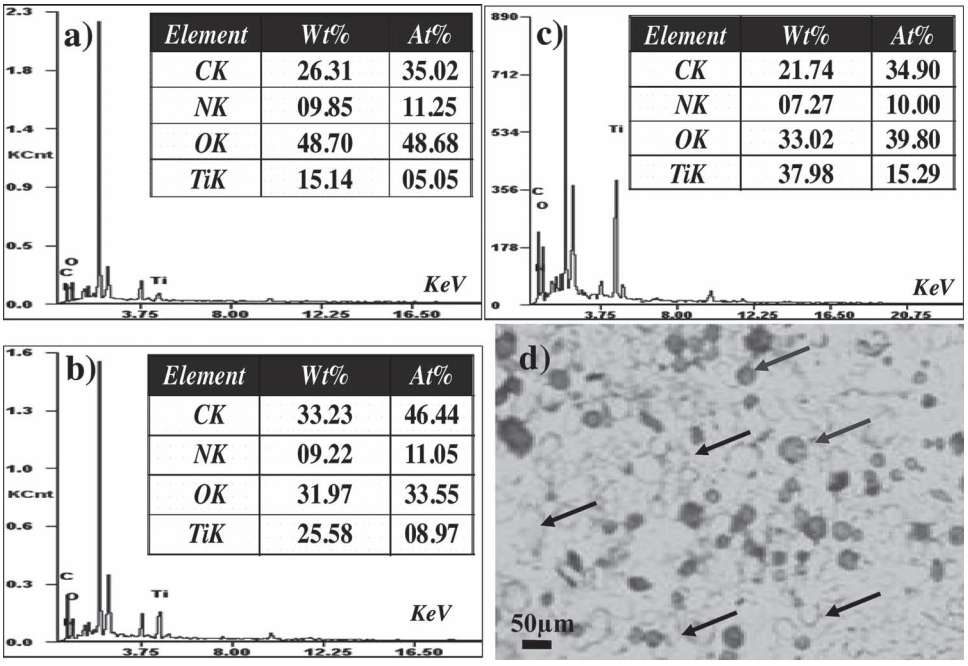

Figure 3. a–c) EDS spectra of the NPSCs: a) NPSCs-1, b) NPSCs-2 and c) NPSCs-3; and d) optical micrograph of NPSCs-4 (scale bar: 50 μm).

2.2. Immobilization of FateDH and FaldDH within/on the NPSCs

In this study, the spatial distribution of two enzymes within/on NPSCs was essential to the efficient construction of the enzyme cascade system. Therefore, to confirm the location of FateDH (the first enzyme), rhodamine B-labeled FateDH was used for the preparation of the NPSCs. A distinct red fluorescence was detected under 543-nm excitation, indicating the presence of FateDH (**Figure 5**a). Furthermore, constant sulfur content on the capsule wall indicated that FateDH was uniformly distributed within the capsule wall as shown in Figure 5b. All the above results confirmed that FateDH had been successfully immobilized within the capsule wall.

In our previous study,[45] we proved that the biomimetic titania could chemically conjugate with enzymes through adduct reaction between catechol groups of oligodopa and amino groups of enzymes.[46] Then, the NPSCs were utilized to conjugate FaldDH (the second enzyme) on the outer surface of the capsule wall (**Figure 6**a).[47–49] In order to avoid interference from FateDH during the characterization of FaldDH-containing NPSCs, the FateDH-free NPSCs were immersed into a FaldDH aqueous solution for two hours. FTIR and EDS spectra were acquired to verify the viable conjugation of FaldDH to the outer surface of the capsule wall. As shown in Figure 6b, the appearance of stretching frequencies from 450 to 700 cm^{-1} was attributed to the typical peaks of titania (Ti-O-Ti).[23] Meanwhile, the peak at around 1650 cm^{-1} could be assigned to absorbance of the amide, suggesting the successful immobilization of FaldDH on the surface of the NPSCs.[23] Furthermore, the absorption peaks located at 2853 cm^{-1} and 2926 cm^{-1} were attributed to -CH_2- and -CH_3, respectively, which should be due to the presence of BuTi and hexadecane. In Figure 6c, the appearance of sulfur in the EDS spectrum also illustrated the successful immobilization of FaldDH. Additionally, the FaldDH loading capacity of NPSCs increased from 45.7 to 192.2 mg g^{-1} (NPSCs) when the concentration of FaldDH increased from 0.1 to 0.5 mg mL^{-1}, as demonstrated in Figure 6d. A slight increase in the loading capacity was observed as the concentration of FaldDH was higher than 0.5 mg mL^{-1}. The FateDH loading capacity of NPSCs was also exploited, and the results were summarized in Figure S3 (Supporting Information). In order to obtain a similar FateDH loading capacity to FaldDH, the FateDH concentration used in the immobilization process was also fixed at 0.5 mg mL^{-1}. The resultant FateDH loading capacity was 168.0 mg g^{-1} (NPSCs).

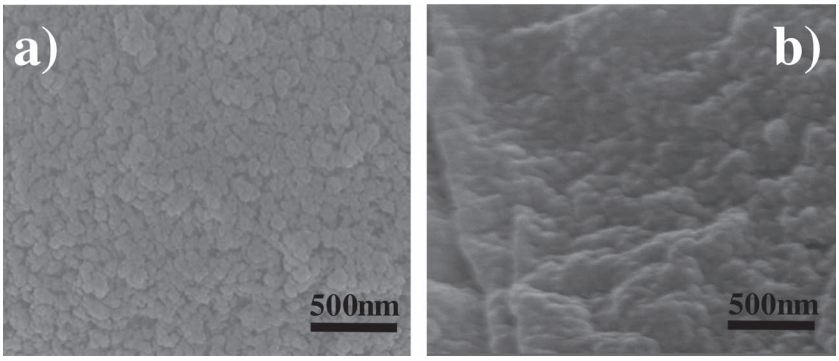

Figure 4. HR-SEM images of a) NPSCs-2 and b) NPSCs-3 (scale bar: 500 nm).

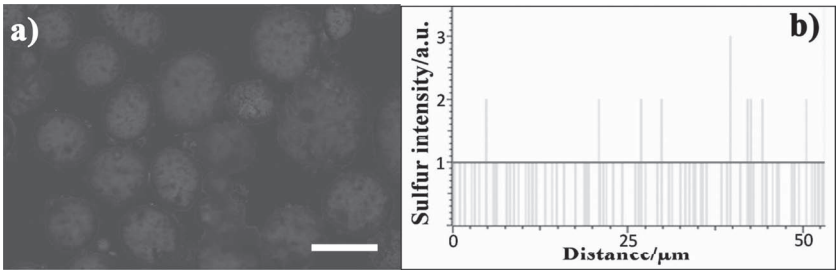

Figure 5. a) Florescence image (scale bar: 50 μm) and b) EDS spectrum of the FateDH-containing NPSCs.

2.3. Catalytic Efficiency and Stability of the Enzyme Cascade System

The enzyme cascade system was applied to convert CO_2 into formaldehyde. Batch reactions were carried out with a similar amount of enzymes (FateDH, 0.37 mg; FaldDH, 0.42 mg), while the concentration of NADH was fixed at 50 mM. For comparison, the catalytic performance of the free enzyme cascade system (FateDH, 0.40 mg; FaldDH, 0.40 mg) and biomimetic titania-based enzyme cascade system (FateDH, 0.37 mg; FaldDH, 0.44 mg) were also evaluated. First, we assayed the formaldehyde yield as a function of the reaction time catalyzed by the free, biomimetic titania- and NPSC-based enzyme cascade systems. **Figure 7**a indicated that the formaldehyde yield increased as the reaction time was prolonged during the 4-h reaction for all three systems. Specifically, the formaldehyde yield of the immobilized systems was higher than that of the free system through the entirety of the 4-h reaction. The immobilized systems exhibited a formaldehyde yield of ≈50.0–60.0% after reaction equilibrium, which was much higher than that of the free system (34.0%). Meanwhile, compared to the free system, the immobilized systems also displayed higher specific activity, especially the initial activity (immobilized systems: 0.79 and 1.53 μmol min^{-1} mg^{-1} vs free system: 0.72 μmol min^{-1} mg^{-1}) (Figure 7b). This observation was in contrary to what was usually expected for the immobilized enzyme for a single step reaction and indicated that the overall equilibrium was shifted favorably toward the product. This interesting phenomenon might be caused by the substantially-reduced diffusion distance that the reaction intermediate travelled between the two enzymes' active sites. The generation of formic acid in the vicinity of the second enzyme (FaldDH) allowed the effective biocatalyzed oxidation of NADH owing to the high local concentration of formic acid.[45,50–52] Another potential explanation for the enhancement of formaldehyde yield was presented in Figure 7c. CO_2 transferred through the outer layer into the particle matrix (or capsule wall) to be converted to formic acid. Therefore, formic acid had to go through the particle matrix (or capsule wall) to escape, which ensured that all of the formic acid molecules fully contacted FaldDH and were converted into formaldehyde.[45,51] Furthermore, it was also found that either the formaldehyde yield or the specific activity of the NPSC-based system was slightly lower than that of the biomimetic titania-based system as shown in Figure 7a,b. The decrease in activity might be attributed to either of the following two causes. First, the high surface area of the carriers could offer more contacting opportunities for enzymes and substrates, resulting in higher enzymatic activity. In our study, compared with the biomimetic titania-based system, the surface area of the NPSC-based system decreased during the construction process, which could explain its reduced activity. Second, when enzymes were in an organic solvent-water mixture, the increased content of organic solvent, especially water-miscible protic and aprotic organic solvent, was capable of removing essential water from the enzyme surface and affecting the polarity of active sites as reported in previous studies.[53–55] Since hexadecane was used and butanol was produced during the formation of Pickering emulsions, the secondary structure of enzyme molecules might be changed. In order to identify the primary reason, the secondary structures of FateDH and FaldDH in the presence of organic solvent were individually characterized by circular dichroism (CD). As illustrated in **Figure 8**a,b, there was little difference between the CD spectra of two enzymes in PBS and in organic solvent-containing PBS (PBS with hexadecane or PBS with a hexadecane-butanol mixture), suggesting a negligible impact of trace organic solvent (V_{oil}/V_{water} = 1/40, V_{BuTi}/V_{oil} = 1/100) on the secondary structure of the two enzymes.[33] Therefore, it can be deduced that hexadecane and butanol did not affect the catalytic activity of FateDH and FaldDH. Finally, it can be concluded that the reduced enzymatic activity was mainly caused by the decreased surface area of the NPSC-based system in comparison to the biomimetic titania-based system.

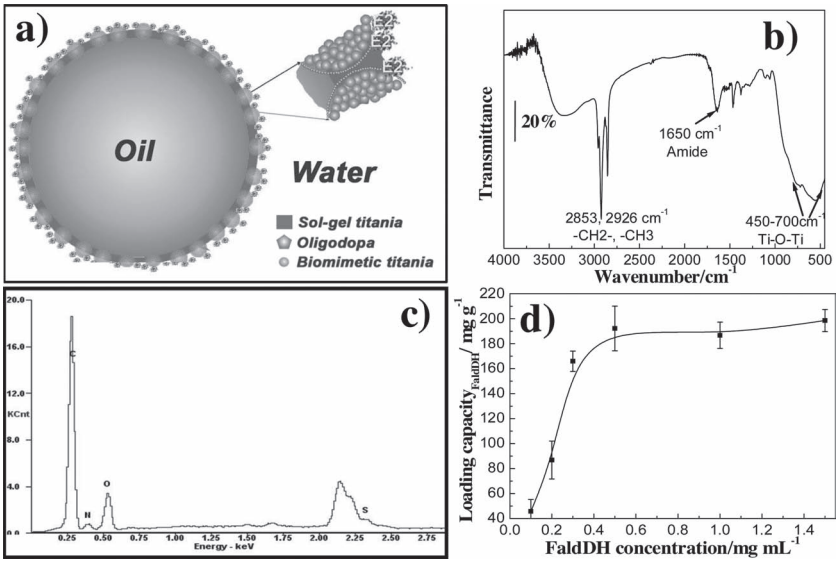

Figure 6. a) Scheme, b) FTIR and c) EDS spectra of the FaldDH-conjugated NPSCs; and d) FaldDH loading capacity of NPSCs as a function of FaldDH concentration.

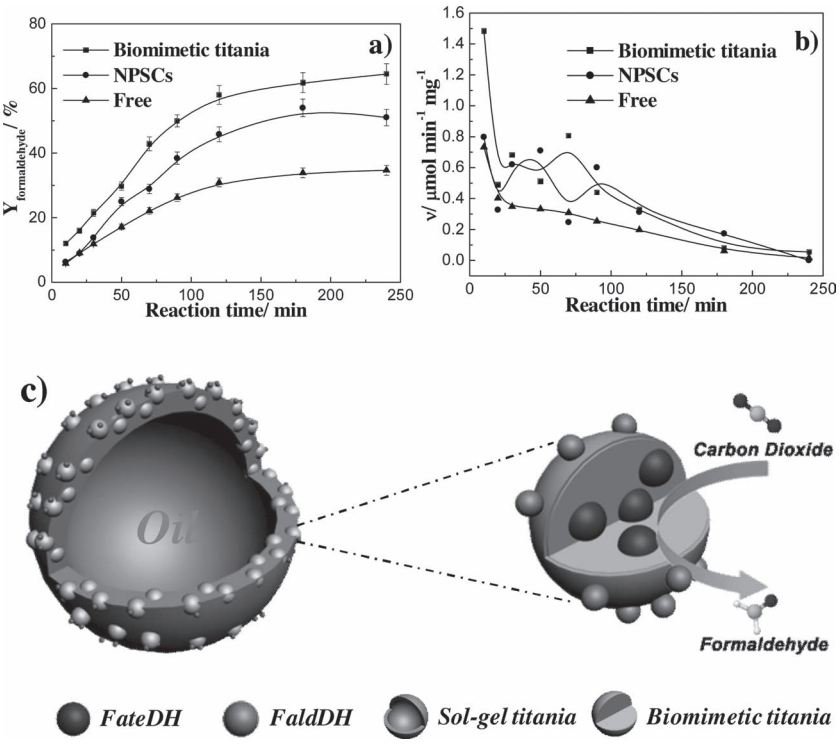

Figure 7. Plots of a) formaldehyde yield and b) specific activity as a function of reaction time for converting CO_2 to formaldehyde of the free, biomimetic titania- and NPSC-based enzyme cascade systems, and c) proposed reaction process of CO_2 to formaldehyde catalyzed by the NPSC-based system.

Subsequently, the structural stability of the NPSC-based system was investigated under moderate stirring after storing at 4 °C over a 30 day period (Figure S5, Supporting Information). Notably, few capsules were deformed or broken. This system retained 80% of its initial activity after storing for 30 days, indicating that the NPSCs could provide a biocompatible and robust microenvironment for both enzymes. Specifically, the relatively small pores of the biomimetic titania[45] and the robust chemical bond between oligodopa and FaldDH could successfully avoid the leakage of two enzymes, retaining their catalytic activity. According to previous reports,[56,57] the loss of enzyme activity would be partially due to the existence of protein-degrading microbe. Therefore, the high retention of enzymatic activity in this study could be partially due to the antibiotic function of titania.[58,59]

2.4. Recycling and Reusing of the Enzyme Cascade System

In the present study, the NPSCs can quickly float to the air/water interface soon after the magnetic stirring or manual shaking was halted (**Figure 9**b,c), which ensured the enzyme cascade system easily recyclable. Before conducting the cascade reaction, the activity and recyclability of FateDH-entrapped NPSCs for converting CO_2 to formic acid were investigated. As shown in Figure 9a, the immobilized FateDH could still convert >89.5% of CO_2 to formic acid after 10 cycles, indicating its excellent activity and recycling stability. For the enzyme cascade reaction of converting CO_2 to formaldehyde, the formaldehyde yield with recycling times of the biomimetic titania- and NPSC-based system was evaluated. As shown in Figure 9d, a continuous decrease of formaldehyde yield was observed in the biomimetic titania-based system as the recycling times increased. This decrease of formaldehyde yield was mostly ascribed to the mass loss of the catalyst during the centrifugation process after each reaction batch.[45] After 10 cycles, only 53.0% of the biomimetic titania was left over, resulting in the decrease of formaldehyde yield from 64.0% to 33.0%. However, the NPSC-based system had superior recyclability as shown in Figure 9b,c. The enzyme recycling efficiency remained almost unaltered after 10 cycles. These results further verified that the NPSCs provided a robust and favorable microenvironment for enzymes.

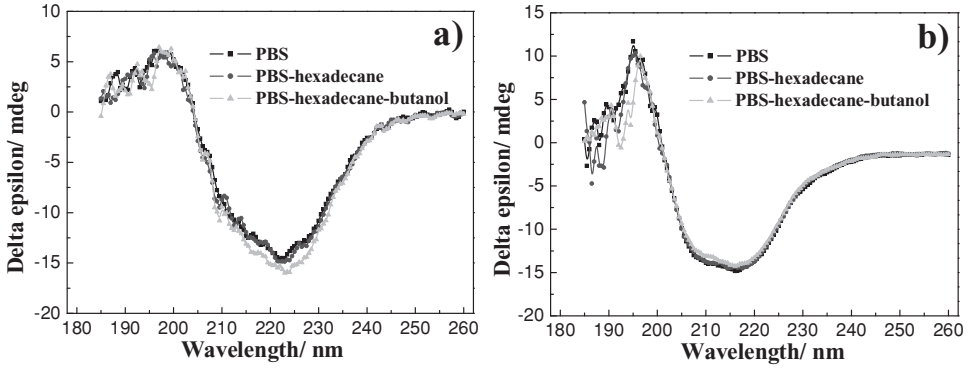

Figure 8. Circular dichroism (CD) spectra of a) FateDH and b) FaldDH dispersed in PBS (50 mM, pH 7.0), PBS (50 mM, pH 7.0) containing hexadecane and PBS (50 mM, pH 7.0) containing a hexadecane-butanol mixture.

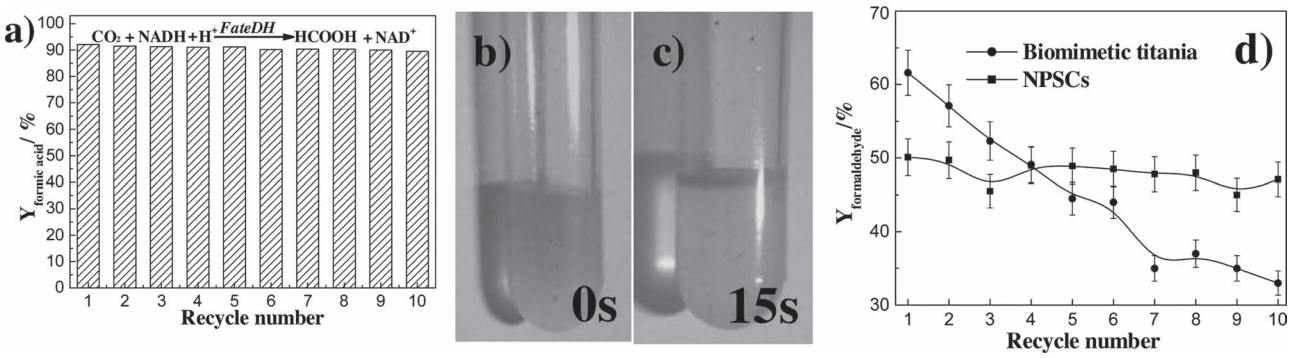

Figure 9. a) Recycling stability of the FateDH-entrapped NPSCs for converting CO_2 to formic acid; b,c) digital photographs of the NPSC-based system spontaneously separable from the bulk solution as the hand shaking stops from b) 0 s to c) 15 s; and d) the recycling stability of the biomimetic titania- and NPSC-based systems.

3. Conclusions

A novel and generic approach combining a Pickering emulsion and sol-gel process has been developed for the facile construction of a NPSC-based enzyme cascade system. Two kinds of enzymes are separately immobilized through physical entrapment within the capsule wall and chemical conjugation onto the surface of the capsules. The robust capsule wall renders the enzyme cascade system with an appropriate microenvironment and superior stability. Meanwhile, the lower density of the oil core than that of water endows the enzyme cascade system with excellent recyclability. Furthermore, the capsule morphology and the enzyme loading capacity can be easily and finely tuned by changing the BuTi/oil ratios and enzyme concentrations. The present approach will be able to evolve as a platform technology to construct novel and efficient nanocatalytic systems for a variety of chemical and enzymatic conversions.

4. Experimental Section

Materials: Titanium(IV) bis(ammonium lactato) dihydroxide (Ti-BALDH, 50 wt% aqueous solution), tris(hydroxymethyl) amiomethane (tris), rhodamine B, formate dehydrogenase from *Candida boidinii* (FateDH, EC.1.2.1.43), formaldehyde dehydrogenase from *Pseudomonas putida* (FaldDH, EC.1.2.1.46), and reduced nicotinamide adenine dinucleotide (NADH, 98 wt%) were purchased from Sigma-Aldrich. 3,4-dihydroxy-L-phenylalanine (dopa) was obtained from Yuancheng Technology Development Co. Ltd. (Wuhan, China). Disodium hydrogen phosphate, sodium dihydrogen phosphate, n-hexadecane, n-butanol, butyl titanate (BuTi), ethanol, hydrochloric acid (HCl) and sodium hydroxide (NaOH) of reagent grade quality were obtained from Guangfu Chemical Co. (Tianjin, China). Arginine was purchased from Bodi Chemical Co. (Tianjin China). Rhodamine B-labeled enzymes were prepared using overnight incubation at room temperature of their mixtures (50 mM phosphate buffer, pH 7.0, protein concentration 1 mg mL^{-1}, [dye]/[enzyme] = 5) followed by exhaustive dialysis (M_W cutoff: 14 000 Da) against phosphate buffer (50 mM, pH 7.0) for 72 h and deionized water for 24 h. All other reagents were of analytical grade and used without further purification. All solutions were prepared using ultrapure water with a resistivity of 182 kΩ m from a Milli Q Plus water purification system (Millipore, Billerica, Massachusetts, USA). The pH values of solutions were measured with a PHS-3C pH-meter (REX Instruments, PHS-3C, Shanghai, China) and adjusted by addition of HCl solution (0.1 M) or NaOH solution (0.1 M). Additionally, the synthesis procedure of oligodopa was illustrated in the Supporting Information.

Preparation of the Oligodopa-Coated Titania Nanoparticles (Biomimetic Titania): A 300 mM aqueous solution of arginine was prepared by dissolving arginine powder in a 50 mM tris-HCl buffer solution (pH 6.8). Then, the synthetic reaction was initiated by adding 0.5 mL Ti-BALDH solution (0.05 M, pH 6.8) into 1 mL arginine solution at ambient conditions. After the reaction continued for 1 min, 0.5 mL of oligodopa solution (2.5 mg mL^{-1} for tris-HCl buffer solution of dopa, pH 7.5) was added to the reaction media. Then the mixture was agitated for another 10.0 min. Finally, the biomimetic titania was obtained after the precipitates were centrifuged at 10 000 rpm and washed more than three times with a 50 mM tris-HCl buffer solution (pH 6.8).

Preparation of the Nanoparticle-Stabilized Capsules (NPSCs): In a typical procedure, 125 µL of hexadecane mixed with a certain amount of BuTi (0, 1.25, 3.75, 6.25, and 12.5 µL) was added into 5 mL of tris-HCl buffer solution (50 mM, pH 6.8) to form a oil-water mixture. Immediately, 2 mg of the biomimetic titania was added into the oil-water mixture followed by emulsification via vigorous shaking for 60 s. (Here, the amount of the biomimetic titania was in accordance with the previous reports to ensure nearly full coverage of NPs on surface of the emulsion drops.)[43] Afterwards, to ensure complete hydrolysis and polycondensation of BuTi, the resultant mixture was gently shaken by test tube shaker for 60 min at ambient conditions. The resultant capsules with 1.25, 3.75, 6.25, and 12.5 µL of BuTi were denoted as NPSCs-1, NPSCs-2, NPSCs-3 and NPSCs-4, respectively.

Preparation of FateDH (the First Enzyme)-Entrapped Biomimetic Titania[45]: 0.5 mg of FateDH was dissolved in 1.0 mL of arginine solution (300 mM, 50 mM tris-HCl buffer solution, pH 6.8). The synthetic reaction was initiated by adding 0.5 mL Ti-BALDH solution (50 mM tris-HCl buffer solution, pH 6.8) into 1 mL arginine solution at ambient conditions. After the reaction continued for 1 min, 0.5 mL of oligodopa solution (2.5 mg mL^{-1} of dopa, 50 mM tris-HCl buffer solution, pH 7.5) was added to the reaction media. Then the mixture was agitated for another 10.0 min. Finally, the FateDH-entrapped biomimetic titania was obtained after the precipitates were centrifuged at 10 000 rpm and washed more than three times with 50 mM tris-HCl buffer solution (pH 6.8). The characterizations of the biomimetic titania with and without enzymes were provided in the Supporting Information (Figure S2 and S4). The FateDH loading capacity of NPSCs was also measured and illustrated in Figure S3 of the Supporting Information.

Construction of the NPSC-Based Enzyme Cascade System: In a typical procedure, 125 µL of hexadecane mixed with 3.75 µL of BuTi was added into the tris-HCl buffer solution (50 mM, pH 6.8). Then 2 mg of the FateDH-entrapped biomimetic titania was added in the mixture followed by emulsification via vigorous shaking for 60 s. Subsequently, the mixture was gentley shaken by test tube shaker for 60 min at ambient conditions. The FateDH-containing NPSCs were spontaneously floated onto the water/air interface in a few seconds after stopping shaking, which were then collected. For immobilizing the second enzyme-FaldDH, FateDH-containing NPSCs were transferred into 1 mL of FaldDH

solution (50 mM tris-HCl buffer solution, pH 7.0) for 2h reaction with continuous shaking under ambient conditions. After siphoning off the buffer solution by using a straw, the NPSC-based enzyme cascade system were obtained and washed more than three times with tris-HCl buffer solution (50 mM, pH 7.0).

For comparison, the enzyme cascade system based on the biomimetic titania was also constructed. Briefly, 2 mg of as-synthesized FateDH-entrapped biomimetic titania was dispersed to 1 mL of FaldDH solution (50 mM tris-HCl buffer solution, pH 7.0) for 2-h reaction with continuous shaking under ambient conditions. Subsequently, the biomimetic titania-based enzyme cascade system was collected through centrifugation at 10 000 rpm for 5 min and washed more than three times with tris-HCl buffer solution (50 mM, pH 7.0).

Enzymatic Conversion of Carbon Dioxide (CO_2) to Formaldehyde: Conversion of CO_2 to formaldehyde was conducted in aqueous solution with free or immobilized enzymes. The whole conversion process involved an initial reduction of CO_2 to formic acid catalyzed by FateDH, followed by reduction of formic acid to formaldehyde by FaldDH. Reduced nicotinamide adenine dinucleotide (NADH) acted as a terminal electron donor for each enzyme-catalyzed reduction. The operating pressure was maintained at 0.3 MPa. The formaldehyde concentration was determined by gas chromatography (GC) equipped with a flame ionization detector (FID; Hewlett-Packard, model HP-6890). All the measurements were repeated three times. It should be mentioned that the formic acid concentration was too low to be detected. Conversion of CO_2 by the biomimetic titania- and NPSC-based systems was performed according to the following procedure. Briefly, immobilized enzymes-containing solution (0.5 mL, 50 mM PBS, pH 7.0) was bubbled with CO_2 for 0.5 h before adding 0.5 mL NADH solution (50 mM PBS, pH 7.0) to initiate the enzyme cascade reaction. The formaldehyde yield (Y,%) calculations were made based on the fact that 1 mole of formaldehyde consumed 2 moles of NADH (Equation (1)).[45,51] The specific activity (v_t, μmol min^{-1} mg^{-1} (enzyme)) was calculated based on Equation (2)

$$Y_{\text{formaldehyhde}} = \frac{2 \times C_{\text{formaldehyhde}}}{C_{\text{NADH,initial}}} \times 100 \quad (1)$$

$$v_t = \frac{V_{\text{system}} \times \left(C_{\text{formaldehyhde},\, t+\Delta t} - C_{\text{formaldehyhde},\, t}\right)}{M_{\text{enzyme}} \times \Delta t} \times 100 \quad (2)$$

where $C_{\text{formaldehyde}}$ was the concentration of formaldehyde after the enzyme cascade reaction (μM), $C_{\text{NADH, initial}}$ was the initial NADH concentration before the enzymatic reaction (μM), V_{system} was the solution volume of the system (L), M_{enzyme} was the total enzyme amount used in this experiment (mg), $C_{\text{formaldehyde, }t+\Delta t}$ was the formaldehyde concentration at the time of $t+\Delta t$ (μM), $C_{\text{formaldehyde, }t}$ was the formaldehyde concentration at the time of t (μM).

Activity Assays of the FateDH-Entrapped NPSCs: Activity assays of the FateDH-entrapped NPSCs were carried out at optimum conditions (pH 7.0, temperature 37 °C, pressure 0.3 MPa).[45,50–52] The enzymatic activity of the FateDH-entrapped NPSCs was evaluated based on the formic acid yield in the reduction of CO_2. 0.5 mL of the FateDH-entrapped NPSCs-containing solution (amount of FateDH: 0.4 mg) was mixed with 0.5 mL of 100 mM NADH solution in 50 mM tris-HCl buffer. To the mixture, CO_2 was then bubbled for 4 h for production of formic acid. A UV-vis spectrophotometer was used for determination of the concentration of NADH in the reaction solution at 340 nm and the yield of formic acid was calculated based on the amount of NADH consumed. The formic acid yield (Y,%) was calculated based on Equation (3):

$$Y_{\text{formic acid}} = \frac{C_{\text{formic acid}}}{C_{\text{NADH, initial}}} \times 100 \quad (3)$$

Where $C_{\text{formic acid}}$ was the concentration of formic acid after the enzyme cascade reaction (μM), $C_{\text{NADH, initial}}$ was the initial NADH concentration before the enzymatic reaction (μM).

Characterization: FTIR spectra of the biomimetic titania and NPSCs were obtained on a Nicolet-6700 spectrometer. 32 scans were accumulated with a resolution of 4 cm^{-1} for each spectrum. HR-SEM images were recorded using a field emission scanning electron microscope (FESEM, Nanosem 430). Elemental analysis was accomplished by energy dispersive spectroscope (EDS) attached to FESEM. TEM observation was performed on a JEM-100CX II instrument. The contact angle analysis was conducted on the membrane surfaces by a contact angle goniometer (JC2000C Contact Angle Meter, Powereach Co., Shanghai, China) at room temperature. Optical and fluorescence microscope images were taken using an Olympus BX51 microscope with a 100× oil immersion objective lens (Olympus, Tokyo, Japan). Changes in the secondary structure of FateDH and FaldDH in the presence of hexadecane or hexadecane-butanol mixture at room temperature were determined by circular dichroism spectroscopy (CD) on a JASCO J715 spectropolarimeter (JASCO, Japan). The enzyme and oil were dispersed in 50 mM phosphate buffer solution (PBS, pH 7.0). The final enzyme concentration was 0.5 g L^{-1} and the volume ratio of water:hexadecane:butanol was 40:1:0.01. Six scans were conducted and averaged for each sample from 185 to 260 nm at a 0.5 nm interval with a rate of 50 nm min^{-1} and a response time of 8 s. The optical path was 1 cm.

Enzyme loading capacity of NPSCs was determined for both enzymes (FateDH and FaldDH). In detail, the loading capacity (μg mg^{-1} (NPSCs)) was calculated according to the Equation (4):

$$\text{Loading capacity}_{\text{FateDH or FaldDH}} = \frac{M_{\text{FateDH or FaldDH, immobilized}}}{M_{\text{NPSCs}}} \quad (4)$$

where $M_{\text{FateDH or FaldDH, immobilized}}$ was the mass of immobilized FateDH or FaldDH (μg), and M_{NPSCs} was the mass of freeze-dried capsules (mg, herein, wet capsules were firstly treated with ethanol to remove the oil core and then freeze-dried). $M_{\text{FateDH or FaldDH, immobilized}}$ was calculated by measuring the concentration of FateDH or FaldDH in the supernatant before and after immobilization (20 ± 2 °C) at 595 nm through Coomassie Blue staining method using a spectrophotometer.

Supporting Information

Supporting Information is available from the Wiley Online Library or from the author.

Acknowledgements

The authors thank the financial support from the National Basic Research Program of China (2009CB724705), National Science Fund for Distinguished Young Scholars (21125627), the National Science Foundation of China (20976127), and the Program of Introducing Talents of Discipline to Universities (B06006).

Received: July 24, 2012
Revised: September 16, 2012
Published online: October 19, 2012

[1] L. Q. Cao, *Curr. Opin. Chem. Biol.* **2005**, *9*, 217.
[2] A. Schmid, J. Dordick, B. Hauer, A. Kiener, M. Wubbolts, B. Witholt, *Nature* **2001**, *409*, 258.
[3] M. Alcalde, M. Ferrer, F. J. Plou, A. Ballesteros, *Trends Biotechnol.* **2006**, *24*, 281.
[4] R. A. Sheldon, *Adv. Synth. Catal.* **2007**, *349*, 1289.
[5] H. J. Kim, M. W. Ruszczycky, S. H. Choi, Y. N. Liu, H. W. Liu, *Nature* **2011**, *473*, 109.

[6] J. B. Siegel, A. Zanghellini, H. M. Lovick, G. Kiss, A. R. Lambert, J. L. S. Clair, J. L. Gallaher, D. Hilvert, M. H. Gelb, B. L. Stoddard, K. N. Houk, F. E. Michael, D. Baker, *Science* **2010**, *329*, 309.
[7] N. K. Navani, Y. F. Li, *Curr. Opin. Chem. Biol.* **2006**, *10*, 272.
[8] G. Liu, Y. Wan, V. Gau, J. Zhang, L. H. Wang, S. P. Song, C. H. Fan, *J. Am. Chem. Soc.* **2008**, *130*, 6820.
[9] A. Zebda, C. Gondran, A. Le Goff, M. Holzinger, P. Cinquin, S. Cosnier, *Nat. Commun.* **2011**, *2*, 370.
[10] S. G. Burton, D. A. Cowan, J. M. Woodley, *Nat. Biotechnol.* **2002**, *20*, 37.
[11] V. V. Mozhaev, M. V. Sergeeva, A. B. Belova, Y. L. Khmelnitsky, *Biotechnol. Bioeng.* **1990**, *35*, 653.
[12] D. Avnir, T. Coradin, O. Lev, J. Livage, *J. Mater. Chem.* **2006**, *16*, 1013.
[13] L. M. Ellerby, C. R. Nishida, F. Nishida, S. A. Yamanaka, B. Dunn, J. S. Valentine, J. I. Zink, *Science* **1992**, *255*, 1113.
[14] H. R. Luckarift, J. C. Spain, R. R. Naik, M. O. Stone, *Nat. Biotechnol.* **2004**, *22*, 211.
[15] A. Pierre, *Biocatal. Biotransform.* **2004**, *22*, 145.
[16] T. K. Jain, I. Roy, T. K. De, A. Maitra, *J. Am. Chem. Soc.* **1998**, *120*, 11092.
[17] L. Betancor, H. R. Luckarift, *Trends Biotechnol.* **2008**, *26*, 566.
[18] F. Cellesi, N. Tirelli, *Colloids Surf., A* **2006**, *288*, 52.
[19] X. Yang, Z. Cai, Z. Ye, S. Chen, Y. Yang, H. Wang, Y. Liu, A. Cao, *Nanoscale* **2012**, *4*, 414.
[20] F. Cellesi, N. Tirelli, *Colloids Surf., A* **2006**, *288*, 52.
[21] R. R. Naik, M. M. Tomczak, H. R. Luckarift, J. C. Spain, M. O. Stone, *Chem. Commun.* **2004**, 1684.
[22] L. Li, Z. Jiang, H. Wu, Y. Feng, J. Li, *Mater. Sci. Eng., C* **2009**, *29*, 2029.
[23] Y. J. Jiang, Q. Y. Sun, Z. Y. Jiang, L. Zhang, J. Li, L. Li, X. H. Sun, *Mater. Sci. Eng., C* **2009**, *29*, 328.
[24] S. Shylesh, V. Schünemann, W. R. Thiel, *Angew. Chem. Int. Ed.* **2010**, *49*, 3428.
[25] P. Torres-Salas, A. del Monte-Martinez, B. Cutiño-Avila, B. Rodriguez-Colinas, M. Alcalde, A. O. Ballesteros, F. J. Plou, *Adv. Mater.* **2011**, *23*, 5275.
[26] B. P. Binks, *Curr. Opin. Colloid Interface Sci.* **2002**, *7*, 21.
[27] S. U. Pickering, *J. Chem. Soc., Trans.* **1907**, *91*, 2001.
[28] Y. Lin, H. Skaff, T. Emrick, A. Dinsmore, T. Russell, *Science* **2003**, *299*, 226.
[29] H. Duan, D. Wang, D. G. Kurth, H. Möhwald, *Angew. Chem. Int. Ed.* **2004**, *43*, 5639.
[30] F. Reincke, S. G. Hickey, W. K. Kegel, D. Vanmaekelbergh, *Angew. Chem. Int. Ed.* **2004**, *43*, 458.
[31] B. P. Binks, R. Murakami, *Nat. Mater.* **2006**, *5*, 865.
[32] J. T. Russell, Y. Lin, A. Böker, L. Su, P. Carl, H. Zettl, J. He, K. Sill, R. Tangirala, T. Emrick, *Angew. Chem. Int. Ed.* **2005**, *44*, 2420.
[33] C. Wu, S. Bai, M. B. Ansorge-Schumacher, D. Wang, *Adv. Mater.* **2011**, *23*, 5694.
[34] T. Chen, P. J. Colver, S. A. F. Bon, *Adv. Mater.* **2007**, *19*, 2286.
[35] H. Strohm, P. Löbmann, *J. Mater. Chem.* **2004**, *14*, 2667.
[36] Y. N. Cui, J. S. van Duijneveldt, *Langmuir* **2012**, *26*, 17210.
[37] G. Jutz, A. Böker, *J. Mater. Chem.* **2010**, *20*, 4299.
[38] Z. Niu, J. He, T. P. Russell, Q. Wang, *Angew. Chem. Int. Ed.* **2010**, *49*, 10052.
[39] Z. Ao, Z. Yang, J. Wang, G. Zhang, T. Ngai, *Langmuir* **2009**, *25*, 2572.
[40] J. Li, A. P. Hitchcock, H. D. H. Stöver, *Langmuir* **2010**, *26*, 17926.
[41] A. Kaiser, T. Liu, W. Richtering, A. M. Schmidt, *Langmuir* **2009**, *25*, 7335.
[42] J. Li, H. D. H. Stöver, *Langmuir* **2010**, *19*, 15554.
[43] C. P. Whitby, D. Fornasiero, J. Ralston, *J. Colloid Interface Sci.* **2010**, *342*, 205.
[44] H. Lee, J. Rho, P. B. Messersmith, *Adv. Mater.* **2009**, *21*, 431.
[45] J. F. Shi, X. L. Wang, Z. Y. Jiang, Y. P. Liang, Y. Y. Zhu, C. H. Zhang, *Bioresour. Technol.* **2012**, *118*, 359.
[46] Y. H. Ren, J. G. Rivera, L. H. He, H. Kulkarni, D. K. Lee, P. B. Messersmith, *BMC Biotechnol.* **2011**, *11*, 63.
[47] L. P. Zhu, J. Z. Yu, Y. Y. Xu, Z. Y. Xi, B. K. Zhu, *Colloids Surf., B* **2009**, *69*, 152.
[48] L. P. Zhu, Y. Y. Xu, Z. Y. Xi, B. K. Zhu, *Acta Polym. Sin.* **2009**, *4*, 394.
[49] H. Lee, J. Rho, P. B. Messersmith, *Adv. Mater.* **2009**, *21*, 431.
[50] R. Obert, B. C. Dave, *J. Am. Chem. Soc.* **1999**, *121*, 12192.
[51] J. F. Shi, L. Zhang, Z. Y. Jiang, *ACS Appl. Mater. Interfaces* **2011**, *3*, 881.
[52] B. El-Zahab, D. Donnelly, P. Wang, *Biotechnol. Bioeng.* **2008**, *99*, 508.
[53] L. Olofsson, I. A. Nicholls, S. Wikman, *Org. Biomol. Chem.* **2005**, *3*, 750.
[54] L. A. S. Gorman, J. S. Dordick, *Biotechnol. Bioeng.* **1992**, *39*, 392.
[55] H. Wehbi, J. Feng, M. F. Roberts, *BBA, Biochim. Biophys. Acta, Biomembr.* **2003**, *1613*, 15.
[56] A. L. Goldberg, *Nature* **2003**, *426*, 895.
[57] A. Goldberg, J. Dice, *Annu. Rev. Biochem.* **1974**, *43*, 835.
[58] B. K. Sunkara, R. D. K. Misra, *Acta Biomater.* **2008**, *4*, 273.
[59] S. Rana, J. Rawat, M. M. Sorensson, R. D. K. Misra, *Acta Biomater.* **2006**, *2*, 421.